The EMBO Journal (2007) 26, 4523–4534 | © 2007 European Molecular Biology Organization | All Rights Reserved 0261-4189/07
www.embojournal.org

THE EMBO JOURNAL

The pro-apoptotic kinase Mst1 and its caspase cleavage products are direct inhibitors of Akt1

Bekir Cinar[1,2], Ping-Ke Fang[1,2], Mohini Lutchman[1,2], Dolores Di Vizio[1,2], Rosalyn M Adam[1,2], Natalya Pavlova[3], Mark A Rubin[4], Pamela C Yelick[5,6] and Michael R Freeman[1,2,3,*]

[1]Urological Diseases Research Center, Department of Urology, Children's Hospital Boston, Boston, MA, USA, [2]Department of Surgery, Harvard Medical School, Boston, MA, USA, [3]Department of Biological Chemistry and Molecular Pharmacology, Harvard Medical School, Boston, MA, USA, [4]Department of Pathology, Brigham and Women's Hospital, Dana Farber Cancer Institute, Harvard Medical School, Boston, MA, USA, [5]Division of Craniofacial and Molecular Genetics, Department of Oral and Maxillofacial Pathology, Tufts University, Boston, MA, USA and [6]Division of Craniofacial and Molecular Genetics, Department of Biomedical Engineering, Tufts University, Boston, MA, USA

Akt kinases mediate cell growth and survival. Here, we report that a pro-apoptotic kinase, Mst1/STK4, is a physiological Akt1 interaction partner. Mst1 was identified as a component of an Akt1 multiprotein complex isolated from lipid raft-enriched fractions of LNCaP human prostate cancer cells. Endogenous Mst1, along with its paralog, Mst2, acted as inhibitors of endogenous Akt1. Surprisingly, mature Mst1 as well as both of its caspase cleavage products, which localize to distinct subcellular compartments and are not structurally homologous, complexed with and inhibited Akt1. cRNAs encoding full-length Mst1, and N- and C-terminal caspase Mst1 cleavage products, reverted an early lethal phenotype in zebrafish development induced by expression of membrane-targeted Akt1. Mst1 and Akt1 localized to identical subcellular sites in human prostate tumors. Mst1 levels declined with progression from clinically localized to hormone refractory disease, coinciding with an increase in Akt activation with transition from hormone naïve to hormone-resistant metastases. These results position Mst1/2 within a novel branch of the phosphoinositide 3-kinase/Akt pathway and suggest an important role in cancer progression.

The EMBO Journal (2007) **26,** 4523–4534. doi:10.1038/sj.emboj.7601872; Published online 11 October 2007
Subject Categories: differentiation & death; molecular biology of disease
Keywords: apoptosis; kinases; lipid rafts; prostate cancer; protein complex

*Corresponding author. Enders Research Laboratories, Department of Urology, Children's Hospital Boston, suite 1161, 300 Longwood Avenue, Boston, MA 02115, USA. Tel.: +1 617 919 2644; Fax: +1 617 730 0238; E-mail: michael.freeman@childrens.harvard.edu

Received: 20 December 2006; accepted: 10 September 2007; published online: 11 October 2007

Introduction

The serine-threonine kinase, Akt1 (protein kinase Bα), is a member of the AGC kinase subfamily, with two close structural relatives, Akt2 and Akt3, encoded by separate genes. The Akt kinases regulate a diversity of cellular events, including cell growth, differentiation and intermediary metabolism by phosphorylating a range of downstream substrates (Cheng *et al*, 2005). Akt kinases are activated by phosphoinositide-3-kinase (PI3K), and are negatively regulated by the lipid phosphatase, PTEN, a tumor suppressor. Inactivating PTEN mutations occur frequently in certain malignancies (Cairns *et al*, 1997; Li *et al*, 1997; Bertram *et al*, 2006) and Akt is frequently activated in tumors (Ayala *et al*, 2004; Majumder and Sellers, 2005). Akt1 mediates cell survival by opposing a variety of apoptotic triggers (Dudek *et al*, 1997; Kulik *et al*, 1997). Although the three Akt paralogs are highly homologous, recent evidence indicates that Akt1 and Akt2 perform unexpectedly distinct roles in tumor cells (Irie *et al*, 2005; Yoeli-Lerner *et al*, 2005). Hyperactivation of Akt1, which stimulates pro-survival mechanisms, also inhibits tumor cell behaviors relevant to metastasis, including motility and invasion through matrix barriers (Irie *et al*, 2005; Yoeli-Lerner *et al*, 2005). In prostate cancer, somatic inactivation of PTEN is common in aggressive tumors and correlates with Akt activation. Inactivation of PTEN in the mouse also leads to Akt activation (Kim *et al*, 2002). Akt substrates include the target of rapamycin complexes, mTORC1 and mTORC2, the FOXO transcription factors, apoptotic signaling proteins, and the tumor suppressor protein TSC2.

Translocation of Akt isoforms to the plasma membrane is an important feature of the activation process. All three Akt family members contain pleckstrin homology (PH) domains that function to relieve kinase autoinhibition by binding to inositol phospholipids. The PH domains are highly conserved in the Akt family, and disruption of phospholipid binding by point mutation of the PH domain results in an inability to activate Akt1 by insulin (Sable *et al*, 1998). Addition of a myristoylation sequence results in constitutive activation of Akt kinase activity (Sable *et al*, 1998). Several positive and negative regulators of Akt, such as PDK1 (Anderson *et al*, 1998), Src (Chen *et al*, 2001), CTMP (Maira *et al*, 2001), and caveolin-1 (Li *et al*, 2003), associate with cytoplasmic membranes (Du and Tsichlis, 2005). However, despite the importance of membrane association for Akt activity, the phosphorylation of Akt by PDK1 (Cho *et al*, 2001), TORC2 (Sarbassov *et al*, 2006), and other kinases (Feng *et al*, 2004), but not membrane localization, is the principal mechanism of kinase activation (Sable *et al*, 1998). The deletion of the PH domain does not inhibit Akt activation by upstream signals, indicating that membrane localization is not required for kinase activity. In fact, ΔPH-Akt1 is a more potent enzyme than wild-type Akt1 (Sable *et al*, 1998). Akt1 can also be activated in the nucleus in a manner that may not depend on association with cytosolic membranes (Trotman *et al*, 2006;

Wang and Brattain, 2006). These observations suggest that the specific physiologic roles played by Akt isoforms may depend on unique strategies for subcellular localization of the kinases as well as their accessory proteins.

Recent evidence suggests that Akt signaling in prostate cancer cells is sensitive to alterations in cholesterol metabolism (Zhuang *et al*, 2002, 2005; Freeman and Solomon, 2004; Adam *et al*, 2007). Cholesterol and glycosphingolipids accumulate in liquid-ordered membrane microdomains, termed 'lipid rafts,' or 'caveolae' in cells that express caveolin proteins. These structures are enriched in certain signaling proteins, such as Src-like kinases. Cholesterol-rich, lipid raft membranes have been implicated in signal transduction, although the mechanistic details of signaling from these microdomains in cancer are still poorly understood (Freeman and Solomon, 2004). The observation that Akt1 is responsive to manipulations that affect lipid raft cholesterol suggests that an Akt subpopulation may be regulated by molecules that transit to or reside within cholesterol-rich membranes.

In this study, we identify the serine-threonine kinase, Mst1/STK4, as a component of an Akt1 multiprotein complex isolated from lipid raft membranes of prostate cancer cells. We show that Mst1 binds to Akt1 directly and functions as an Akt inhibitor, preferentially in lipid rafts. Mst1 is pro-apoptotic in its active form (de Souza and Lindsay, 2004); thus, a role as an Akt1 inhibitor is consistent with the described function of the kinase as an amplifier of apoptotic signals. Interestingly, however, we demonstrate that Mst1 inhibits Akt1 in its mature, full-length form, and also in its caspase-cleaved state, where two distinct species localize to the cytoplasm and the nucleus, respectively, and are independently capable of attenuating Akt1 activity. Patterns of protein expression seen in human tumors suggest that Mst1 may play a role in prostate cancer progression.

Results

Mst1/STK4 is an Akt1-interacting protein

Biochemical fractionation of LNCaP prostate cancer cells using a method that enriches for cholesterol-rich, lipid raft membranes (Solomon *et al*, 1998), followed by analysis of Akt1 by western blot with putatively monospecific antibodies, indicated that Akt1 resides primarily in the Triton X-100 (TX-)-soluble fraction (Supplementary Figure S1A). (In this study, Akt rather than Akt1 is used in the text and figures if specificity against the Akt1 isoform is not assured.) These experiments and others using sucrose gradient centrifugation to isolate lipid raft membranes indicate that about 10% of non-nuclear Akt1 is present in lipid raft fractions (Adam *et al*, 2007). Blotting and immunoprecipitation (IP) experiments showed that a protein that was unlikely to be Akt, but which formed a complex with Akt in TX-insoluble, octylglucoside (OCG)-soluble fractions (Figure 1A and Supplementary Figure S1A), was recognized by a polyclonal antibody (9275, Cell Signaling Technology) raised against one of the principal Akt1 phosphorylation sites (p-T308). We inferred this to be a crossreaction, because this protein was not recognized by a monoclonal antibody against the p-T308 Akt1 residue. We hypothesized that Akt forms a complex with another kinase, apparently preferentially in a raft-like subcellular location.

To identify the proposed Akt interaction partner, we immunoprecipitated Akt from TX-insoluble/OCG-soluble fractions from LNCaP cells and used mass spectrometry to identify and characterize co-precipitating proteins. These

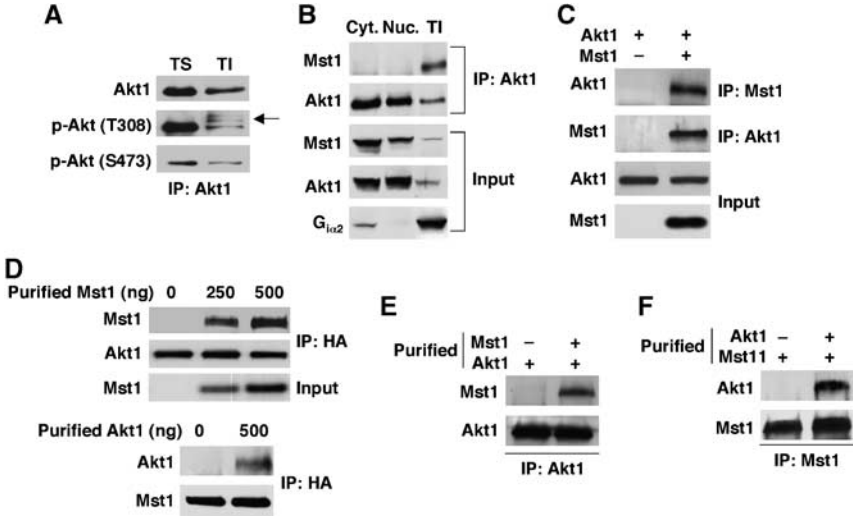

Figure 1 Endogenous Mst1 and Akt1 interaction in Triton-X-100-insoluble subcellular fractions. (**A**) p-T308-reactive protein(s) co-precipitate with Akt1 from lipid raft-enriched (TI) fractions. Akt1 was immunoprecipitated and blots were generated with antibodies to total Akt, p-T308 and p-S473. TS = Triton X-100-soluble fraction. (**B**) Mst1 and Akt1 interact principally in detergent-insoluble fractions. Akt1 was immunoprecipitated from cytoplasmic (Cyt), nuclear (Nuc), and TI fractions prepared from LNCaP cells. Input shows protein levels before IP. Data are representative of two individual experiments. (**C**) Full-length Mst1 forms a complex with Myr-Akt1. Cell lysates were immunoprecipitated with anti-Mst1- or anti-Akt1-specific antibody. (**D**) Dose-dependent interaction of purified Mst1 with Myr-Akt1. Myr-Akt1 transiently expressed in HEK 293T cells was immunoprecipitated with anti-HA antibody. Upper panels: immune complexes were incubated with the indicated amounts of purified Mst1 and resolved by SDS–PAGE. Immunoblots are against Mst1 and Akt1. Lower panels: the reciprocal experiment, showing interaction of purified Akt1 with Mst1 in HEK 293T cells (500 ng Akt1). (**E, F**) Protein-binding assay with purified Akt1 and Mst1. Purified Akt1 was precipitated with anti-Akt1 antibody and subsequently incubated with or without purified Mst1. In the reciprocal experiment, purified Mst1 was precipitated with anti-Mst1 antibody and then incubated with or without purified Akt1.

experiments identified the serine-threonine kinase, Mst1/STK4, as a component of the precipitated complex (Supplementary Figure S1B). The presence of Mst1 in the Akt complex used for IP and mass spectrometry was confirmed by western blot (Supplementary Figure S1C). Immunoblotting was also used to confirm that the 9275 anti-p-T308 antibody recognized purified Mst1 (Supplementary Figure S1D and E).

Because Mst1 was identified in a lipid raft-enriched fraction, we tested whether endogenous Mst1/Akt complexes could be found in other subcellular fractions. Mst1 was detected primarily in Akt complexes of TX-insoluble fractions (Figure 1B), despite the fact that Akt predominantly localized to cytosolic and nuclear fractions, whereas Mst1 was most abundant in the cytosolic fraction. The identification of Akt1 as the Akt isoform interacting with Mst1 was confirmed using an Akt1-specific antibody (2H10, specificity demonstrated in Supplementary Figure S1F). These observations suggest that complex formation between endogenous Mst1 and Akt1, as measured by co-IP using two different Akt1 antibodies, occurs preferentially in lipid raft membrane fractions.

Mst1 also co-precipitated from HEK 293T cells with myristoylated (membrane-targeted and constitutively active) Akt (Myr-Akt1) using Akt antibodies, and conversely, Myr-Akt1 co-precipitated with Mst1 antibodies (Figure 1C). Mst1 also interacted with wild-type (non-myristoylated) Akt1 (Supplementary Figure S2A). In addition, co-precipitation of Akt1 and Mst1 was observed in COS cells (Supplementary Figure S2B).

Mst1 and Akt1 physically interact

To determine whether Mst1 and Akt1 interact directly, myristoylated Akt1 was immunoprecipitated in the presence of increasing amounts (0, 250, and 500 ng) of purified Mst1, and the presence of Mst1 in the precipitated complex was assessed. Mst1 interacted with Akt1 in a dose-dependent manner (Figure 1D, upper panels). In a separate experiment, purified Mst1 interacted with endogenous Akt1 immunoprecipitated from HEK 293T cells (Supplementary Figure S2C). Conversely, purified Akt1 interacted with overexpressed full-length Mst1 (Figure 1D, lower panels). In addition, we performed direct binding assays using the two purified proteins. For these experiments, baculovirus-expressed Akt1 was immunoprecipitated with anti-Akt1 antibody, and then mixed with purified Mst1. Similarly, purified Mst1 was immunoprecipitated with anti-Mst1 antibody and then mixed with purified Akt1. Both experiments demonstrated complex formation between Mst1 and Akt1 (Figure 1E and F).

The two Mst1 caspase cleavage products bind within the Akt1 hydrophobic domain

Mst1 has two principal functional domains: an N-terminal kinase domain that is released from an inhibitory C-terminal regulatory domain by a caspase-dependent mechanism during apoptosis (de Souza and Lindsay, 2004). To determine which Mst1 domain interacts with Akt1, we generated two deletion constructs, Mst1-N (residues 1–330) and Mst1-C (residues 331–487), corresponding to the two principal caspase cleavage products (Graves *et al*, 2001). Each construct was coexpressed with either Myr-Akt1 or T7-tagged wild-type Akt1. Surprisingly, both Mst1-N-terminal and Mst1-C-terminal domains interacted with both forms of Akt1 (Figure 2A and B), in a manner indistinguishable from full-length Mst1. Complex formation between Mst1-N and Myr-Akt1 was competitively inhibited by Mst1-C (Figure 2C), and similarly, complex formation between Mst1-C and Myr-Akt1 was inhibited by Mst1-N (Supplementary Figure S2D), consistent with the conclusion that both principal Mst1 domains interact with Akt1 independently and at a common binding region.

In contrast, a kinase-dead (KD) Mst1 mutant, K59R (Yamamoto *et al*, 2003), did not interact with Myr-Akt1 (Figure 2D). Dosage experiments demonstrated that coexpression of the Mst1-KD mutant with wild-type Mst1 dramatically inhibited the ability of wild-type Mst1 to bind to Akt1 (Figure 2E, upper panels). The KD mutant also dose-dependently inhibited the kinase activity of the immunoprecipitated Mst1 complex (Figure 2E, lower panels). These data are most easily explained by the sequestration of wild-type Mst1 by Mst1-K59R into an inactive complex, consistent with the dominant inhibitory function of the KD mutant (Yamamoto *et al*, 2003). These results suggest that conversion of full-length Mst1 into an active form may be required for formation of the Akt1/Mst1 complex.

In contrast to the results observed using full-length Mst1-K59R, the inactive N-terminal caspase cleavage product containing the K59R mutation (Mst1-N (K59R), Cheung *et al*, 2003) did interact with Myr-Akt1 (Figure 2F). These data suggest that the Mst1 phosphotransferase function, while required for conversion of inactive Mst1 to the active form, is not required for binding of Mst1 to Akt1. Consistent with this interpretation, Mst1-C, which does not harbor kinase activity, also bound Akt1 (Figure 2B).

We analyzed a series of Akt1 mutants to identify structural features required for interaction with Mst1 (Figure 3). Akt1 has three major functional domains: an N-terminal PH domain, a highly conserved catalytic domain and a C-terminal hydrophobic motif. Phosphorylation at two sites (T308 and S473) is required for full kinase activity. Myc-tagged Mst1 was coexpressed in HEK 293T cells along with the HA-tagged Akt1 mutants, as shown in Figure 3A. Co-IP revealed that the construct lacking the PH domain maintained the interaction with Akt1 (Figure 3B), indicating that the membrane-associated region is not essential for Akt1 binding. However, two constructs with mutations near the C-terminus, P424A/427A, and S473A, bound poorly or not at all to Akt1 (Figure 3B). The weak binding seen with the S473A mutant cannot be attributed to reduced kinase activity resulting from ablation of one of the principal phosphorylation sites because of the fact that two other kinase-inactivating point mutations (T308A and K179M), which lie outside the C-terminal region and individually ablate all kinase activity (Alessi *et al*, 1996; Dudek *et al*, 1997), did not inhibit binding to Akt1 (Figure 3C). Similarly, use of the PI3K inhibitor, LY294002, which also inhibits Akt, stimulated the Mst1–Akt1 interaction and also increased the amount of phosphorylated (activated) Mst1 recoverable in the precipitated Mst1/Akt1 complex (Figure 3D). Together, these data demonstrate that Akt1 kinase activity is not required for Mst1 binding. Notably, the P424A/427A mutations reside within the Src-binding site, and these P→A substitutions result in a loss of Src binding (Jiang and Qiu, 2003). This suggests that the Mst1-binding site on Akt1 is within the C-terminal region, which serves as a binding domain for several proteins that regulate Akt1 activity (Du and Tsichlis, 2005). Consistent with this prediction,

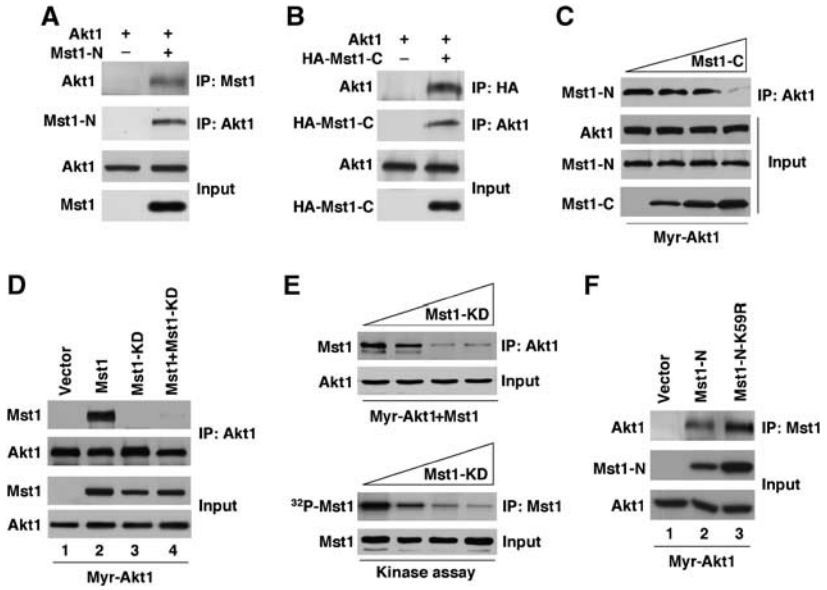

Figure 2 Mst1-N and Mst1-C interaction with Akt1. (**A**) Interaction of Akt1 with Mst1-N. Myr-Akt1 was transiently expressed in the absence or presence of Mst1-N in HEK 293T cells. Akt1 or Mst1 was immunoprecipitated and immune complexes were blotted with the reciprocal antibody. (**B**) Interaction of Akt1 with Mst1-C. T7-tagged Akt1 was transiently expressed in the absence or presence of HA-Mst1-C in HEK 293T cells. (**C**) Competition experiments. Myc-Mst1-N and Myr-Akt1 were coexpressed with increasing amounts (0, 2, 3, and 4 μg) of Myc-Mst1-C. Akt1 was immunoprecipitated and the presence of Myc-Mst1-N in Akt1 immune complexes assessed with anti-Myc antibody. (**D**) Co-precipitation of HA-Mst1 or kinase dead Mst1-K59R or Mst1-N-K59R, and Myr-Akt1. Lysates from HEK 293T cells transiently expressing wild type or Mst1-K59R and Myr-Akt1 were immunoprecipitated anti-Akt1 antibody. (**E**) Dose-dependent inhibition of Mst1–Akt1 interaction and Mst1 complex *in vitro* kinase activity by dominant-negative Mst1 (K59R). Upper panels: competition experiments (upper panels). Myc-Mst1 and Myr-Akt1 were transiently coexpressed with increasing amounts (0, 0.5, 1, and 2 μg) of Mst1-K59R in HEK 293T cells. Lysates expressing wild type, Mst1-K59R, and Myr-Akt1 were immunoprecipitated with anti-Akt1 antibody. Lower panels: Mst1 complex kinase activity. Mst1 was immunoprecipitated from lysates with anti-Myc antibody subjected to kinase assay using radioactive ^{32}P-γ-ATP, followed by autoradiography. (**F**) Co-precipitation of HA-Mst1-N or kinase dead Mst1-N-K59R, and Myr-Akt1. Lysates from HEK 293T cells expressing Mst1-N or Mst1-N-K59R and Myr-Akt1 were immunoprecipitated with anti-Mst1 antibody.

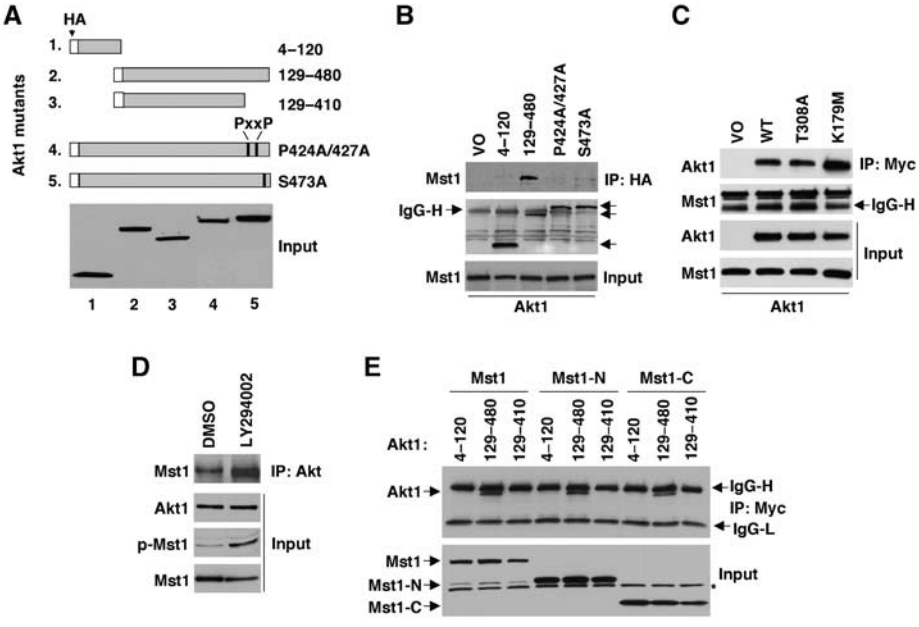

Figure 3 Mst1 and caspase-cleaved Mst1 fragments interact with the Akt1 C-terminal region. (**A**) HA-Akt1 truncation and point mutants used for experiments in (B) and (E). (**B**) Co-precipitation of HA-Akt1 mutants with Myc-Mst1. Akt1 mutants were co-transfected with Myc-Mst1 in HEK 293T cells. Co-IP was performed with anti-HA antibody. Arrows on the right identify the relative location of Akt1 reactive bands. (**C**) Lysates from HEK 293T cells expressing wild-type Myc-Mst1 and wild-type Akt1, the phosphorylation site mutant Akt1-T308A, or the ATP-binding site mutant Akt1-K179M were immunoprecipitated with anti-Myc antibody and blotted for Akt1. Data in all panels are representative of at least two individual experiments. IgG heavy (H) chain is indicated. (**D**) Co-precipitation of Akt1 with Mst1. HEK 293T cells were co-transfected with Mst1 and Myr-Akt1, followed by treatment with PI3K inhibitor (LY294002; 20 μM) or vehicle (DMSO) for 60 min. Co-precipitation assay was performed in lysate. (E) Co-precipitation of Myc-tagged Mst1, Mst1-N, and Mst1-C with Akt1 truncation mutants. Mst1, Mst1-N, and Mst1-C were coexpressed with Akt1 mutants in HEK 293T cells. * Indicates nonspecific band. IgG heavy (H) and light (L) chains are indicated.

deletion of 70 amino acids at the Akt1 C-terminus abolished binding (Figure 3E). Both Mst1-N and Mst1-C demonstrated a similar requirement for the C-terminal region for binding, indicating that both caspase cleavage fragments bind to the same region in Akt1 as does full-length Mst1, consistent with the results of the competition experiments (Figure 2C and Supplementary Figure S2D).

Mst1 colocalizes with activated Akt1

Mst1 has been demonstrated to shuttle between the cytoplasm and nucleus (Ura *et al*, 2001). To assess the extent of subcellular Akt1 and Mst1 colocalization *in vivo*, Mst1 was expressed either alone, or together with (constitutively active) Myr-Akt1, in COS cells (Figure 4A). Immunofluorescence microscopy revealed that in the absence of Myr-Akt1, Mst1 was present in both the nucleus and cytoplasm. Myr-Akt1 and Mst1 extensively colocalized at membrane sites, as assessed by labeling with the cholera toxin B subunit (CTxB), which recognizes a lipid raft-resident ganglioside (GM1) (Nichols, 2003). A similar result was seen using GFP-Myr-Akt1 in DU145 cells (Supplementary Figure S3A). In contrast, in the presence of GFP-Myr-Akt1, the kinase-inactive Mst1-K59R mutant was not demonstrably present at raft-like membranes (Supplementary Figure S3A). Consistent with these data, endogenous Mst1 was found in lipid raft-enriched fractions in DU145 cells by western blot (Supplementary Figure S3B); however, the pattern of distribution between raft and non-raft cytosol/membranes fractions resembled that seen for Akt1.

Coexpression experiments carried out with Mst1-N and Mst1-C in DU145 cells indicated that Mst1-C colocalized with GFP-Myr-Akt1 in the cytoplasm and at the plasma membrane, whereas Mst1-N markedly did not colocalize with the membrane-targeted form of Akt1 (Figure 4B). Consistent with the above finding, in LNCaP cells, where Akt1 is constitutively activated (Cairns *et al*, 1997), Mst1-N colocalized with endogenous p-Akt in nuclei, whereas Mst1-C colocalized with p-Akt in the cytoplasm and plasma membrane (Figure 4C). Mst1 also colocalized with Akt1 following treatment of DU145 cells with IGF-1, a physiologic Akt1 activator (Figure 4D). In these experiments, Mst1/Akt1 complexes were identifiable by IP when Myr-Akt1 and Mst1 were overexpressed (Supplementary Figure S3C).

Mst1 antagonizes Akt1 activity in mammalian cells

Mst1 and its closely related paralog, Mst2, exert pro-apoptotic functions by antagonizing cell survival signals (Deng *et al*, 2003; de Souza and Lindsay, 2004; O'Neill *et al*, 2004). To investigate whether either Mst1 or Mst2 act on endogenous Akt1, Mst1 and Mst2 were depleted in LNCaP cells by RNA interference, and Akt1 activity was evaluated (Figure 5A and E). Depletion of either Mst1 or Mst2 quantitatively increased Akt1 phosphorylation and activity levels relative to the scrambled siRNA negative controls. Interestingly, depletion of both proteins further enhanced Akt1 activity (Figure 5A), indicating that endogenous Mst1 and Mst2 cooperate in LNCaP cells to negatively regulate Akt1. Neither the scrambled nor the Mst1/2 siRNAs had any effect on Akt1 protein levels.

Forced expression of full-length Mst1, Mst1-N or Mst1-C inhibited endogenous Akt1 activity in LNCaP cells with similar efficiency (Figure 5B) and induced apoptosis (Figure 5C), consistent with the requirement for constitutive signaling through the PI3K/Akt pathway for survival in this cell line (Lin *et al*, 1999). Knockdown of Mst1, Mst2, or both isoforms (Mst1/2) antagonized the apoptotic effect of LY294002 in LNCaP cells, implicating endogenous Mst1 in the apoptotic mechanism induced by PI3K inhibition (Figure 5D).

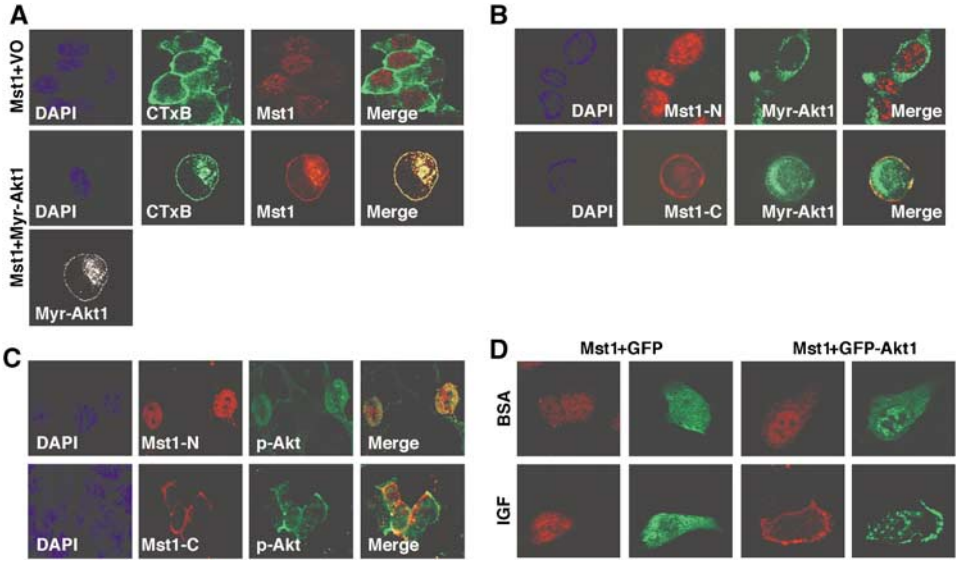

Figure 4 Immunofluorescent localization of Mst1 and Akt1. (**A**) Colocalization of Mst1 and Myr-Akt1 in COS cells. Confocal images of cells co-transfected with full-length HA-Mst1 and Myr-Akt1 or vector only (VO). Mst1 (Cy3, red) or Akt1 (Cy5, purple; shown here as pseudocolored 'white'). Nuclei (DAPI, blue); lipid raft membranes (GM1, cholera toxin B (CTxB; green). (**B, C**) Localization of Mst1-N and Mst1-C, and GFP-Myr-Akt1 coexpressed in DU145 cells (B). Colocalization of Mst1 truncation mutants with endogenous phospho-Akt in LNCaP cells (C). (**D**) Relocalization of HA-Mst1 in response to Akt1 activation by IGF-1. DU145 cells were co-transfected with Mst1 (Cy3, Red) and GFP vector only or GFP-Akt1. After starvation, cells were treated with IGF (50 ng/ml) or BSA control. Data in (A–D) are representative of three individual experiments.

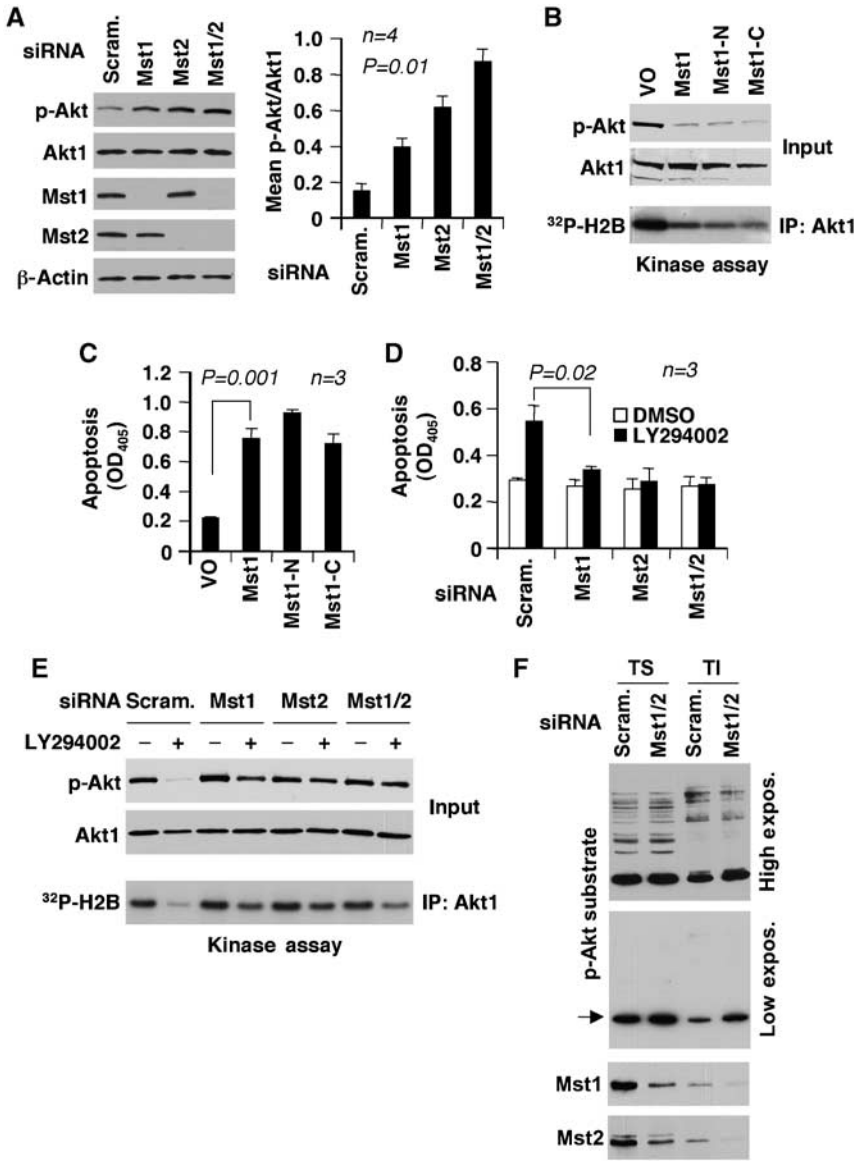

Figure 5 Mst1 antagonizes Akt1 signaling. (**A**) Knockdown of Mst1, Mst2, or Mst1/2 increases Akt phosphorylation (p-S473). LNCaP cells were transfected with a pool of siRNA oligos (100 nM) targeting Mst1 or Mst2. Scrambled siRNA oligos were a negative control. Lysates were prepared 48 h after transfection. The graph shows normalized signal intensity. (**B**–**D**) Mst1 inhibition of Akt activity and Mst1-mediated apoptosis in LNCaP cells. Mst1, Mst1-N, and Mst1-C constructs were expressed for 36 h (B, C). Mst1, Mst2, or Mst1 and Mst2 (Mst1/2) were knocked down for 36 h, followed by treatment with LY294002 (20 μM) or DMSO for 60 min (D, **E**). Cell death was measured using cells grown overnight under serum-free conditions. Akt phosphorylation (S473) and kinase activity in (B) (blots) and (D) were determined in lysates. (**F**) The effects of Mst1/2 knockdown on Akt substrate phosphorylation. Mst1 and Mst2 were knocked down for 36 h. Detergent-soluble (TS) and lipid raft-enriched (TI) fractions were prepared from Mst1/2 or control (scrambled pool) siRNA-transfected LNCaP cells. Phosphorylated Akt substrates were recognized by phospho-Akt substrate antibody.

As expected, endogenous Akt1 activity was substantially inhibited in LY294002-treated LNCaP cells transfected with a scrambled oligo pool; however, Akt1 inhibition was modest when Mst1, Mst2, or Mst1/2 were silenced (Figure 5E). Mst1/2 knockdown also resulted in the differential increase in phosphorylation within lipid raft-enriched fractions of a likely Akt substrate, recognized by an antibody raised against a phosphorylated Akt consensus site (compare lipid raft-enriched (TI) and non-lipid raft cytosolic fractions (TS), Figure 5F), suggesting that Mst1/2 may function preferentially within lipid raft membranes. An inhibitor of the JNK pathway did not attenuate the ability of Mst1 to inhibit Akt1 (Supplementary Figure S4), indicating that JNK, which can be activated by Mst1 (Glantschnig *et al*, 2002), is not involved in the mechanism we describe here. These observations indicate that endogenous Mst1/2 regulate endogenous Akt, and that both kinases appear to be involved in the apoptotic process induced by disruption of the PI3K/Akt pathway in LNCaP cells.

Mst1 is activated by staurosporine (Ura *et al*, 2001). We observed robust Mst1 phosphorylation in response to staurosporine in MC3T3 cells; consequently, we attempted to capture the dynamic formation of Mst1/Akt1 complexes during staurosporine-induced apoptosis in these cells. Complexes between full-length Mst1 and Akt1, and cleaved Mst1-N and Akt1, were identified in staurosporine-treated

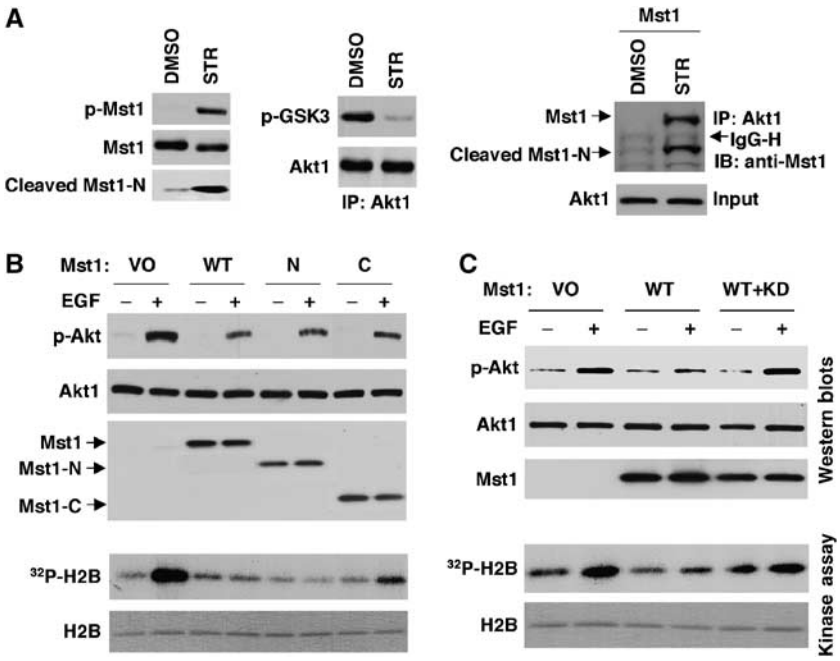

Figure 6 Mst1–Akt complex formation and inhibition of EGF-induced Akt activity. (**A**) MC3T3 cells were treated with 100 nM staurosporine (STR) or DMSO vehicle for 3 h. Akt1 was immunoprecipitated from lysates and subjected to kinase assay. Relative Akt1 kinase activity was determined by immunoblotting of IP eluates with antibodies to phosphorylated GSK3 (p-GSK3α/β) and Akt. Inputs were blotted with antibodies to total and phosphorylated Mst1 to confirm STR-induced phosphorylation of Mst1. Right panel: co-precipitation of endogenous Akt1 with exogenous Mst1. MC3T3 cells were transfected with Mst1. At 24 h, cells were treated with STR or DMSO. Co-precipitation assay was performed in lysate. (**B, C**) Endogenous Akt1 is inhibited by wild-type Mst1, Mst1-N, and Mst1-C. COS cells were transfected with respective plasmids. Cells were stimulated with EGF (20 ng/ml) or vehicle for 10 min under serum-free conditions. Akt phosphorylation and kinase activity were determined in lysates. Dominant negative (Mst1-KD) inhibits the effect of Mst1 on Akt1 activity (C).

MC3T3 cells transfected with full-length Mst1 (Figure 6A). These data show that Mst1/Akt1 complexes may include both full-length and N-terminal caspase-cleaved Mst1 forms.

Our findings to this point suggested that all three forms of Mst1—full-length, and N- and C-terminal caspase cleavage products—are Akt1 inhibitors. Transfection experiments in COS cells demonstrated that full-length Mst1, as well as Mst1-N and Mst1-C, inhibited EGF-stimulated endogenous Akt phosphorylation and kinase activity (Figure 6B). Inhibition was abolished by co-transfection with the KD Mst1-K59R mutant (Figure 6C), indicating that Akt1 inhibition originates from Mst1. Taken together, these data demonstrate that Mst1 and its two caspase cleavage products inhibit Akt1 activity, most likely by a mechanism involving complex formation between the two proteins.

Mst1 reverts an Akt1-induced phenotype in vivo, in the zebrafish

To determine whether Mst1 can inhibit Akt1 *in vivo*, we have taken advantage of the fact that genes can be easily overexpressed in the zebrafish (*Danio rerio*) embryo by cRNA injection at the single-cell stage. We observed that injection of human *MYR-AKT1* cRNAs into single-cell stage zebrafish embryos resulted in a prominent gastrulation defect clearly evident at 24 h (Figure 7), consistent with a previous report on the effect of constitutively activated Akt1 in early zebrafish development (Chan *et al*, 2002). Coinjection of human *MST1* cRNAs resulted in the rescue of the *MYR-AKT1*-induced phenotype (Figure 7), demonstrating that, as *in vitro*, Mst1 can functionally antagonize activated Akt1 *in vivo*. These experiments were repeated extensively, to confirm a dose–response relationship between the amount of injected human *MST1* cRNA and phenotypic rescue (Table I, experiment A). In contrast, injection of cRNA encoding the full-length kinase-inactive *MST1* mutant (K59R) did not rescue the Akt1-induced phenotype (Figure 7; Table I, experiment A), consistent with the observation that the K59R mutation in full-length Mst1 resulted in loss of Akt1 binding and loss of Akt inhibitory activity.

The zebrafish cRNA injection assay also allowed us to examine the effects of the Mst1-N and Mst1-C cleavage products on Akt1 activity in an *in vivo* setting. Coinjections of single-cell zebrafish embryos with *MST1-N* or *MST1-C* cRNAs along with *MYR-AKT1* cRNA showed that both truncated Mst1 forms were able to rescue the Myr-Akt1-induced phenotype in a manner indistinguishable from that of the full-length *MST1* cRNA (Figure 7; Table I, experiment B). This assay also allowed us to test the prediction that inactive Mst1-N (K59R) would inhibit Akt1 *in vivo*, based on the fact that Mst1-N KD mutant bound Akt1, unlike full-length Mst1-K59R (Figure 2F). This prediction was confirmed in the zebrafish, where coinjection of *MST1-N* (K59R) cRNA rescued the Myr-Akt1 phenotype (Figure 7; Table I, experiment B). In summary, consistent with the biochemical analyses, results from the *in vivo* studies in zebrafish indicate that Mst1 kinase activity is required for conversion of full-length Mst1 into an Akt1 inhibitor, and that the kinase activity *per se* is not required for inhibition of Akt1 by Mst1. This is consistent with published data that Mst1 is largely inactive in non-apoptotic cells and requires an activating event to become fully functional (de Souza and Lindsay, 2004).

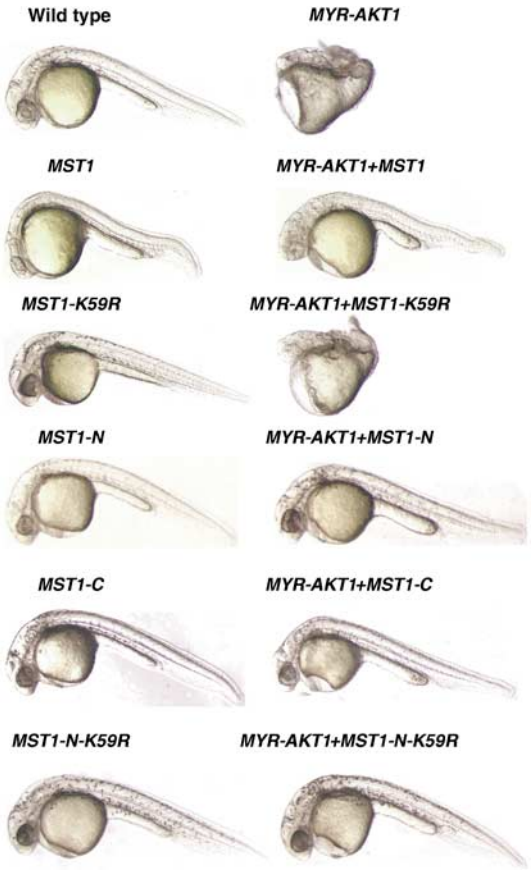

Figure 7 Mst1 inhibits Akt1 in zebrafish development. Injection of *MST1*, *MST1-KD* (K59R), *MST1-N*, *MST1-C*, or *MST1-N* (K59R) cRNA alone or together with *MYR-AKT1* cRNA into single-cell stage zebrafish embryos. Data were collected 24 h post-fertilization. Data are representative of multiple injections. Results are presented in Table I (experiments A and B).

Mst1 and Akt1 expression in human prostate cancer

Signaling through the PI3K/Akt pathway has been demonstrated to be important in prostate cancer and other malignancies (Ayala *et al*, 2004; Cheng *et al*, 2005). To characterize Mst1 expression during prostate cancer progression, and to determine how any such changes might correlate with changes in Akt1 expression, slides from a human prostate cancer tissue microarray (TMA) were immunohistochemically stained with well-characterized antibodies. This TMA contains specimens corresponding to benign prostate, localized adenocarcinoma, and hormone naïve and hormone refractory metastatic cancer. Mst1 and Akt1 localized to identical subcellular compartments in adjacent sections (Figure 8A and B), suggesting that cell-trafficking mechanisms in the tumor cells are permissive for direct interaction between the two proteins. Mst1 and Akt1 levels both increased from the normal to the malignant state, and both declined in the metastatic cancers (Figure 8C and D). Mst1 protein levels in the cancer group declined quantitatively with disease progression. High levels of activated Akt (p-S473) corresponded to the lowest levels of Mst1 seen in the tissues (Figure 8E and F), suggesting that inhibitory effects of Mst1/2 on Akt activity may diminish in some cases with progression to advanced disease in prostate cancer.

Table I *MYR-AKT1*, *MST1*, and *MST1* truncation mutant cRNA injections and rescue

	% Phenotypic	% Rescue	No. injected
Experiment A. MYR-AKT1 and MST1 cRNA injection and rescue			
25 ng/μl of *MYR-AKT1**	100	NA	89
25 ng/μl of *MYR-AKT1* + 25 ng/μl of *MST1*†	75	25	28
25 ng/μl of *MYR-AKT1* + 50 ng/μl of *MST1***	27	73	283
25 ng/μl of *MYR-AKT1* + 50 ng/μl of *MST1-K59R**	100	0	166
50 ng/μl of *MST1*	0	NA	116
50 ng/μl of *MST1-K59R*	0	NA	222
Experiment B. MYR-AKT1 and MST1 truncation mutants and rescue			
50 ng/μl of *MYR-AKT1**	100	NA	95
50 ng/μl of *MYR-AKT1* + 50 ng/μl of *MST1-N*†	0	100	47
50 ng/μl of *MST1-N*†	0	NA	62
50 ng/μl of *MYR-AKT1* + 75 ng/μl of *MST1-C*†	63	37	71
75 ng/μl of *MST1-C*	0	NA	55
50 ng/μl of *MYR-AKT1* + 100 ng/μl of *MST1-N-K59R***	60	40	108
100 ng/μl of *MST1-N-K59R*	0	NA	74

χ^2 statistical analysis. $P<0.001$ between * and † group, between * groups and ** group, and between † and ** group.

Discussion

In this study, we show that the serine-threonine kinase, Mst1/STK4, is a novel inhibitor of Akt1. The regulatory mechanism has a number of interesting features that have not been previously described. Mst1 was originally identified as a highly active kinase during cellular apoptosis and is now known as a caspase target and an amplifier of apoptotic signals (Ura *et al*, 2001; Cheung *et al*, 2003; de Souza and Lindsay, 2004). We identified Mst1 by mass spectrometry in an immunoprecipitated Akt complex generated from lipid raft-enriched biochemical fractions isolated from LNCaP cells. We found that, in comparison to cytosolic and nuclear fractions, lipid raft fractions were a favored site of interaction between the endogenous Mst1 and Akt1 proteins, suggesting that association of the complex with lipid rafts was biologically significant. Consistent with this interpretation, in cells expressing Myr-Akt1, a form of Akt1 that is heavily overrepresented in lipid raft membranes (Adam *et al*, 2007), Mst1 relocated primarily to the cytosolic regions that were decorated with a lipid raft marker. RNA silencing of Mst1/2 also resulted in a differential increase, within lipid rafts, in the phosphorylation of a prominent protein recognized by an Akt substrate antibody and therefore likely to be a downstream target of Akt1. Thus, Mst1 appears to be an Akt1 regulator that, in part, functions within cholesterol-rich membranes.

We demonstrate that full-length Mst1, as well as its two major caspase cleavage products consisting of the N-terminal and C-terminal regions of Mst1, function as Akt1 inhibitors by a mechanism that likely involves direct interaction with Akt1. Consistent with this interpretation, baculovirus-purified Akt1 and Mst1 formed a complex *in vitro* in the absence of accessory proteins. Mst1-N and Mst1-C do not share significant homology at the level of primary

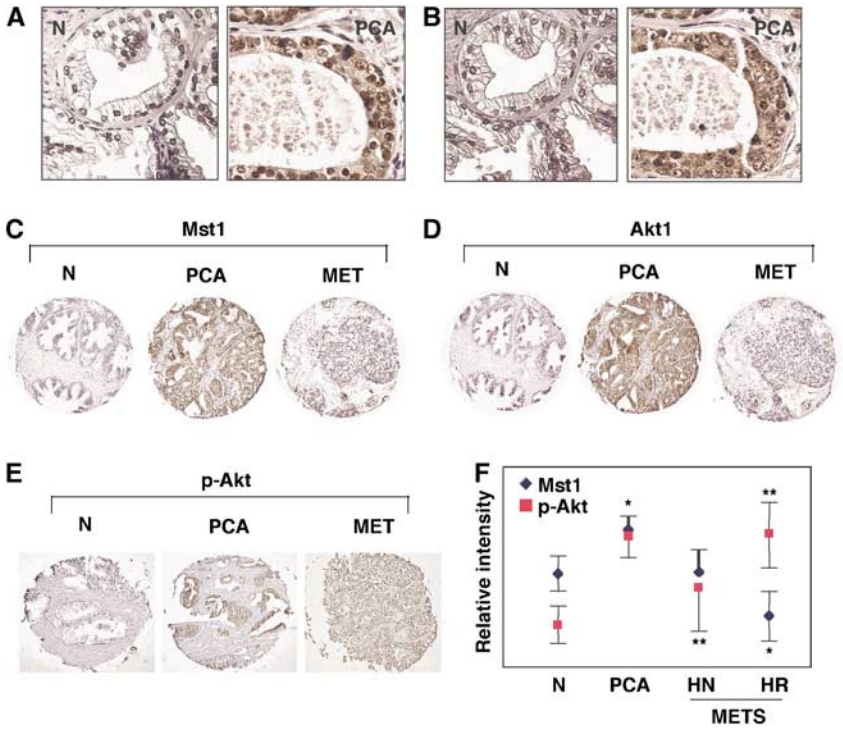

Figure 8 TMA analysis of Mst1 and Akt1 expression in human prostate tissues. (**A, B**) High magnification of Mst1 (A) and Akt1 (B) immunostaining, showing similar subcellular localization. (**C, D**) Selected images of TMA cores showing immunohistochemical staining of Mst1 (A) and Akt1 (B) in prostate cancer progression. The micrographs are representative of quantitative data obtained by ChromaVision analysis. (**E**) Selected TMA cores showing immunhistochemical staining with p-Akt (S473) antibody. MET, metastasis; PCA, organ confined prostate cancer. (**F**) Relative intensities of Mst1 and p-Akt as assessed by ChromaVision. Benign tissue (N, $n=18$), prostate adenocarcinoma (PCA, $n=36$), hormone naive (HN) metastases ($n=19$), hormone refractory (HR) metastases ($n=17$). $^{*}P\leqslant 10^{-6}$, $^{**}P\leqslant 10^{-3}$. Error bars denote 95% confidence intervals.

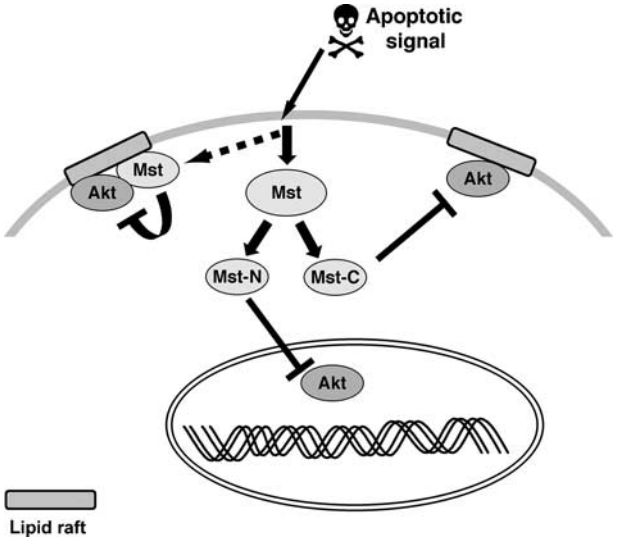

Figure 9 A model illustrating Mst1/2 inhibition of Akt. Mst1/2 and Akt reside in an endogenous complex in cholesterol-rich, lipid raft membranes. Following activation of an apoptotic signal, cytosolic and possibly lipid raft-residing Mst1/2 inhibit Akt. Mst1 caspase cleavage products bind to and inhibit Akt in the cytoplasm and nucleus. Association of Mst1/2 with activated Akt may provide a rapid means of inhibiting the PI3K/Akt pathway during apoptosis and/or providing negative feedback when Akt is activated.

sequence. Although several kinases are targeted by caspase cleavage (Widmann *et al*, 1998), and in some cases are functionally re-directed following caspase-dependent proteolysis (Schlesinger *et al*, 2002), this is the first example of a kinase having two structurally unrelated domains whose cleaved products act in a fashion similar to the mature protein. For example, in contrast to Mst1, another membrane-localized Akt1 inhibitor, PRK2, only binds to Akt1 in its cleaved form (Koh *et al*, 2000). It is possible that non-cleaved Mst1 serves to regulate Akt1 as a component of a pre-existing complex that can respond rapidly to upstream signals, and that Mst1 activation and cleavage occurs within this complex. In support of this model, Mst1 has been shown to exist in complex with other functional regulators, such as the tumor suppressor protein, RASSF1A, which plays a role in death receptor signaling (Oh *et al*, 2006) and mitosis (Guo *et al*, 2007).

Our results suggest that the N-terminal caspase product, Mst1-N, which is a mediator of chromatin condensation during apoptosis (Ura *et al*, 2001; Cheung *et al*, 2003), assumes multiple roles following transit to the nucleus, and that Mst1-C, which is involved in autoinhibition of full-length Mst1 (Praskova *et al*, 2004), plays an additional role as a cytosolic Akt1 regulator following caspase cleavage. Mst1-N has previously been shown to localize primarily to nuclei, whereas Mst1-C was demonstrated to reside in the cytoplasm and at cell membranes (Ura *et al*, 2001), and our data are consistent with this conclusion. However, we also show that full-length Mst1 can colocalize with activated Akt1 when Akt1 is targeted to cytosolic membranes. These findings suggest that both the full-length forms of the protein, as well as the caspase-cleaved fragments, regulate Akt1 within different regions of the cell, possibly as components of larger

complexes that reside in distinct subcellular compartments. A model consistent with our findings is shown in Figure 9.

We have employed a variety of complimentary approaches to demonstrate that Mst1 and its N- and C-terminal forms inhibit Akt1, including a novel functional assay in the zebrafish embryo. Because Myr-Akt1 is approximately 60-fold more active than wild-type Akt1 (Andjelkovic *et al*, 1997), the results of the zebrafish experiments strongly suggest that Mst1 and its cleaved fragments are potent Akt1 inhibitors. The zebrafish studies also allowed us to verify that both Mst1 cleavage products inhibit Akt1 in a manner that depends on direct binding, not intrinsic phosphotransferase activity. Our finding that KD-Mst1-N can bind and inhibit Akt1, while mature KD-Mst1 cannot do either, is consistent with the described mechanism of Mst1/2 activation, which involves intramolecular phosphorylation of Thr183 (Thr180 in Mst2) within the activation loop, thereby converting the protein from an inactive to an active configuration (Praskova *et al*, 2004). Taken together, our results strongly suggest that kinase-inactive, uncleaved Mst1 cannot inhibit Akt1, because intrinsic phosphotransferase activity is required for autoactivation of the protein. Once activated, binding of Mst1 to Akt1 is sufficient to inhibit Akt1 phosphorylation, activity and downstream signaling events. This model allows for the possibility that Akt1 and Mst1 may be associated in a 'latent' form in a multiprotein complex and that upstream signals may specify the onset or extent of inhibitory activity (Figure 9).

We found that all three forms of Mst1 require the C-terminal region of Akt1 for binding. Consistent with these results, the membrane-associated Akt1 inhibitor, CTMP, also reportedly functions by a mechanism involving direct binding to this region, thereby preventing Akt1 phosphorylation (Maira *et al*, 2001). Mst1-N shares sequence homology with the Akt1-binding region of another Akt1 inhibitor, PRK2, which is also cleaved by caspases during apoptosis (Supplementary Figure S5) (Koh *et al*, 2000), although the Akt1-binding region of PRK2 does not contain a kinase domain. Direct binding of an inhibitor to the Akt1 hydrophobic region may thus be an economical means of regulating kinase activity by limiting the ability of PDK1 to phosphorylate T308 in the activation loop.

Our data also indicate that Mst1 and Mst2 are endogenous Akt1 inhibitors in LNCaP cells. Knockdown of either Mst paralog also reduced the apoptotic effect of PI3K inhibition in LNCaP cells, demonstrating that Mst1/2 mediate apoptosis in this background. Mst2 likely serves a functional role similar to Mst1. For example, an important feature of the pro-survival mechanism of the kinase Raf-1 is the suppression of Mst2 (O'Neill *et al*, 2004). We found that Mst1 and Akt1 colocalize in human prostate cancer tissues and expression levels of the two kinases in the TMA we examined were altered in a similar pattern with disease progression. Importantly, we found that Mst1 levels declined with progression to hormone refractory disease and this decline coincided with an increase in Akt phosphorylation, consistent with the possibility of a regulatory relationship. An interesting hypothesis that remains to be tested is whether reduction in Mst1/2 expression contributes to the emergence of the metastatic phenotype, possibly due to loss of the proteins' apoptotic function.

Our study demonstrates that Akt1 intersects directly with the Mst1 pathway, thus illuminating another branch of the PI3K/Akt signal transduction mechanism. The Mst1/2 homologs, STE20 in *Saccharomyces cerevisiae* and Hippo in *Drosophila* are mediators of programmed cell death, indicating a high degree of evolutionary conservation of the apoptotic function (Udan *et al*, 2003). The PI3K/Akt pathway has an ancient evolutionary history (Cho *et al*, 2001), and the Akt inhibitory function of human Mst1 and its cleavage products is conserved *in vivo* as seen in the zebrafish model. These findings suggest that the Mst/Akt regulatory relationship may be evolutionarily conserved.

Materials and methods

Plasmids

RNA isolation and reverse transcription (RT) were performed as described previously (Cinar *et al*, 2001). Human Mst1 cDNA was generated by PCR using a high-fidelity system (Invitrogen, Carlsbad, CA). Human Mst1, Mst1-N, and Mst1-C were cloned by PCR into pCMV-HA or pCMV-Myc. For cRNA generation, Mst1, Mst1-N, and Mst1-C were cloned by PCR into pCR2II, from which sense and antisense RNA transcripts were derived. The pCMV6-HA-Myr-Akt1 (mouse) plasmid was from Thomas Franke, Columbia University, and pcDNA3-T7-Akt1 was from William Sellers, Dana-Farber Cancer Institute. HA-Akt truncation mutants and HA-Akt-PXXP were from Carol Lange, University of Minnesota. Additional HA-Akt1 constructs were generated by PCR. GFP-Akt1 was obtained as described previously (Skaletz-Rorowski *et al*, 2003). Point mutations were generated using the Quick-change kit (Stratagene, La Jolla, CA). Nucleotide sequencing was used to confirm the sequence of all constructs.

Antibodies and reagents

Mst1, p-Mst1 (T183), Akt, p-Akt (T308/S473), and phospho-Akt1 substrate antibodies were purchased from Cell Signaling (Danvers, MA); anti-HA was obtained from Covance (Berkeley, CA); anti-Myc was obtained from BD Biosciences (Mountain View, CA); Cy-3 or Cy5-labeled secondary antibodies were obtained from Jackson ImmunoResearch (West Grove, PA); JNK and PI3K inhibitors and staurosporine were purchased from Calbiochem (San Diego, CA); purified Akt1 and Mst1 were purchased from Upstate Biotechnology (Lake Placid, NY); FITC-CTxB was purchased from Sigma (St Louis, MO); SuperSignal was obtained from Pierce (Rockford, IL); Lipofectamine 2000 was purchased from Invitrogen; Fugene-6 was purchased from Roche. (Indianapolis, IN); Dharma*FECT* 2 was obtained from Dharmacon Inc. (Lafayette, CO); and IGF-1 and EGF were obtained from R&D Systems (Minneapolis, MN).

Immunoprecipitation and western blotting

Fractionations were performed as described previously (Zhuang *et al*, 2005). Cell lyses were performed in buffer containing 20 mM HEPES, pH 7.4, 150 mM NaCl, 0.5% NP-40, 1 mM EDTA, and protease inhibitors. For immunoprecipitation, cleared lysates were incubated with antibody overnight at 4°C. Antibody–antigen complexes were collected on Protein A- or G-sepharose. Immunoprecipitates were resolved by SDS–PAGE, transferred to nitrocellulose membranes and blocked either with PBST (0.1% Tween-20) containing 5% (w/v) skim milk powder or PBST containing 5% BSA (Sigma). Following immunoreactions, signals were visualized by chemiluminescence.

Mass spectrometry

Akt immune complexes were fractionated by SDS–PAGE and proteins visualized with SyproRuby. Excised gel fragments were destained, then dehydrated in 100% MeCN, dried, rehydrated with 200 μl trypsin solution (20 ng/μl in 40 mM NH_4HCO_3/10% MeCN, pH 8.1), and incubated overnight at 37°C. Following digestion, fragments were extracted with 50% MeCN/5% trifluoroacetic acid. Extracts were dried and clarified with ZipTip C_{18} columns (Millipore Corporation, Billerica, MA). Digests were eluted and spotted directly onto MALDI plates. Mass spectra were generated using a Voyager-DE Pro workstation (Applied Biosystems; Foster City, CA) in reflector mode. Spectra were internally calibrated and smoothed using Data Explorer (Applied Biosystems), and submitted

to either Mascot (Matrix Science Ltd) or Protein Prospector (UC San Francisco). Refinements of peptide mass data were performed by iterative recalibration and resubmission to the above databases.

Cell culture and transfections

LNCaP and DU145 cells were cultured in RPMI medium. HEK 293T and COS cells were grown in DMEM medium. MC3T3 cells were cultured in α-MEM. Media were supplemented with 10% FBS and 1% penicillin/streptomycin. Cells were incubated at 37°C/5% CO_2. Lipofectamine 2000 or Fugene-6 was used to perform cell transfections with plasmids.

Immunocytochemistry and microscopy

Cells were plated on eight-well tissue culture slides at 70% confluence. Individual wells were transfected with 100 ng DNA. Cells were fixed in 3% paraformaldehyde for 30 min at room temperature before antibody labeling. The following probes were used: FITC-CTxB (20 ng/ml); anti-phospho (S473)-Akt antibody (1:100), goat anti-rabbit Cy-5 antibody (1:100 dilution); anti-Mst1 polyclonal antibody (1:50), Cy3 goat-anti-rabbit (1:100). Cells were imaged at ×63 with a Plan-Apochromat oil immersion lens on either an Axioplan 2 Apotome epifluorescence microscope (Zeiss, Germany) or an LSM 510 confocal microscope (Zeiss).

The human prostate TMA, developed at Brigham and Women's Hospital, is composed of 97 quadruplicate samples of human normal and tumor prostate tissue: benign (25), localized cancers distributed across Gleason sum categories (36), hormone naïve metastases (19), and hormone-resistant metastases (17). These cases are from well-fixed specimens. All samples were collected with Institutional Review Board approval. Paraffin sections were mounted on glass slides and baked at 60°C for 1 h, de-waxed, and processed for antigen retrieval. Slides were incubated 12 h at 4°C with primary antibodies, used at the following empirically determined dilutions: anti-Mst1 rabbit polyclonal antibody (1:50) or with Akt1 mouse monoclonal antibody (2H10, 1:100); and phospho-Akt (Ser473, 3787S, from Cell Signaling Technology) rabbit monoclonal antibody (1:50). Sections were incubated with HRP-conjugated anti-rabbit IgG for 30 min at room temperature, chromogen solution was applied and the reaction monitored at the microscope. Nuclei were counterstained with hematoxylin. The ACIS system (ChromaVision, San Juan Capistrano, CA) was used for quantitative analysis.

RNAi, kinase and cell death assays

siRNAs were obtained from Dharmacon. Transfections were performed using Dharma*FECT* 2 reagent. For *in vitro* Akt kinase reactions, Akt immune complex was incubated at 30°C for 30 min with H2B (1 μg per reaction) and 10 μCi ^{32}P-γ-ATP or 100 μM unlabeled-ATP. The reaction mixture was run on SDS–PAGE and autoradiographed. Cell death assays were performed using the Cell Death Detection kit (Roche, Basel, Switzerland).

Zebrafish assays

Human *MYR-AKT1*, *WT MST1*, *MST1-K59R*, *MST1-N*, *MST1-N-K59R*, and *MST1-C* cRNAs were transcribed with mMESSAGE mMACHINE (Ambion Inc., Austin, TX). The reactions were carried out at 37°C for 2 h, followed by digestion with RNase-free DNase for 30 min. Transcribed and capped cRNAs were tailed and purified using the Poly(A) Tailing Kit and the MEGAclear Purification Kit (Ambion Inc., Austin, TX). The final cRNA products were precipitated, dissolved in DNase-free/RNase-free water, and quantitated. Single-cell cRNA injections were performed as described previously by us (Albertson *et al*, 2005). Injections (1–3 pl/injection) were titrated at 25, 50, 75, and 100 ng cRNA/ml to determine the lowest *MYR-AKT1* cRNA concentration producing a consistent phenotype, and the lowest *MST-1* variant cRNA concentration for rescue experiments. Based on the results of these titrations, *MYR-AKT1* cRNAs were injected at concentrations of 25 and 50 ng/μl, and *MST-1* variant cRNAs were used at 25, 50, and 75 ng/μl.

Statistical analysis

Values are expressed as mean ± s.d. Where appropriate, an unpaired *t*-test was conducted to analyze for differences between treatments. Independent-samples *t*-test was performed to evaluate significance using the TMA. χ^2-test was used to assess significance in the zebrafish studies. Statistical significance was set at $P \leqslant 0.05$.

Supplementary data

Supplementary data are available at *The EMBO Journal* Online (http://www.embojournal.org).

Acknowledgements

We acknowledge the excellent technical assistance of Paul Guthrie, Francesca Demichelis, Christopher Lafargue, and Robert Kim. We also thank Jonathan Chernoff, X Sean Li, Nishit Mukhopadhyay, and Thomas Roberts for helpful comments. This study was supported by NIH R37 DK47556, R01 CA112303, P50 DK65298, and US Army DAMD17-03-2-0033 (MRF), the AUA Foundation and US Army postdoctoral fellowship DOD W81XWH-04-1-0295 (BC), and the American-Italian Cancer Foundation (DDV).

References

Adam RM, Mukhopadhyay NK, Kim J, Di Vizio D, Cinar B, Boucher K, Solomon KR, Freeman MR (2007) Cholesterol sensitivity of endogenous and myristoylated Akt. *Cancer Res* **67:** 6238–6246

Albertson RC, Payne-Ferreira TL, Postlethwait J, Yelick PC (2005) Zebrafish acvr2a and acvr2b exhibit distinct roles in craniofacial development. *Dev Dyn* **233:** 1405–1418

Alessi DR, Andjelkovic M, Caudwell B, Cron P, Morrice N, Cohen P, Hemmings BA (1996) Mechanism of activation of protein kinase B by insulin and IGF-1. *EMBO J* **15:** 6541–6551

Anderson KE, Coadwell J, Stephens LR, Hawkins PT (1998) Translocation of PDK-1 to the plasma membrane is important in allowing PDK-1 to activate protein kinase B. *Curr Biol* **8:** 684–691

Andjelkovic M, Alessi DR, Meier R, Fernandez A, Lamb NJ, Frech M, Cron P, Cohen P, Lucocq JM, Hemmings BA (1997) Role of translocation in the activation and function of protein kinase B. *J Biol Chem* **272:** 31515–31524

Ayala G, Thompson T, Yang G, Frolov A, Li R, Scardino P, Ohori M, Wheeler T, Harper W (2004) High levels of phosphorylated form of Akt-1 in prostate cancer and non-neoplastic prostate tissues are strong predictors of biochemical recurrence. *Clin Cancer Res* **10:** 6572–6578

Bertram J, Peacock JW, Fazli L, Mui AL, Chung SW, Cox ME, Monia B, Gleave ME, Ong CJ (2006) Loss of PTEN is associated with progression to androgen independence. *Prostate* **66:** 895–902

Cairns P, Okami K, Halachmi S, Halachmi N, Esteller M, Herman JG, Jen J, Isaacs WB, Bova GS, Sidransky D (1997) Frequent inactivation of PTEN/MMAC1 in primary prostate cancer. *Cancer Res* **57:** 4997–5000

Chan J, Bayliss PE, Wood JM, Roberts TM (2002) Dissection of angiogenic signaling in zebrafish using a chemical genetic approach. *Cancer Cell* **1:** 257–267

Chen R, Kim O, Yang J, Sato K, Eisenmann KM, McCarthy J, Chen H, Qiu Y (2001) Regulation of Akt/PKB activation by tyrosine phosphorylation. *J Biol Chem* **276:** 31858–31862

Cheng JQ, Lindsley CW, Cheng GZ, Yang H, Nicosia SV (2005) The Akt/PKB pathway: molecular target for cancer drug discovery. *Oncogene* **24:** 7482–7492

Cheung WL, Ajiro K, Samejima K, Kloc M, Cheung P, Mizzen CA, Beeser A, Etkin LD, Chernoff J, Earnshaw WC, Allis CD (2003) Apoptotic phosphorylation of histone H2B is mediated by mammalian sterile twenty kinase. *Cell* **113:** 507–517

Cho KS, Lee JH, Kim S, Kim D, Koh H, Lee J, Kim C, Kim J, Chung J (2001) *Drosophila* phosphoinositide-dependent kinase-1 regulates apoptosis and growth via the phosphoinositide 3-kinase-dependent signaling pathway. *Proc Natl Acad Sci USA* **98:** 6144–6149

Cinar B, Koeneman KS, Edlund M, Prins GS, Zhau HE, Chung LW (2001) Androgen receptor mediates the reduced tumor growth, enhanced androgen responsiveness, and selected target gene

transactivation in a human prostate cancer cell line. *Cancer Res* **61:** 7310–7317

de Souza PM, Lindsay MA (2004) Mammalian Sterile20-like kinase 1 and the regulation of apoptosis. *Biochem Soc Trans* **32:** 485–488

Deng Y, Pang A, Wang JH (2003) Regulation of mammalian STE20-like kinase 2 (MST2) by protein phosphorylation/dephosphorylation and proteolysis. *J Biol Chem* **278:** 11760–11767

Du K, Tsichlis PN (2005) Regulation of the Akt kinase by interacting proteins. *Oncogene* **24:** 7401–7409

Dudek H, Datta SR, Franke TF, Birnbaum MJ, Yao R, Cooper GM, Segal RA, Kaplan DR, Greenberg ME (1997) Regulation of neuronal survival by the serine-threonine protein kinase Akt. *Science* **275:** 661–665

Feng J, Park J, Cron P, Hess D, Hemmings BA (2004) Identification of a PKB/Akt hydrophobic motif Ser-473 kinase as DNA-dependent protein kinase. *J Biol Chem* **279:** 41189–41196

Freeman MR, Solomon KR (2004) Cholesterol and prostate cancer. *J Cell Biochem* **91:** 54–69

Glantschnig H, Rodan GA, Reszka AA (2002) Mapping of MST1 kinase sites of phosphorylation. Activation and autophosphorylation. *J Biol Chem* **277:** 42987–42996

Graves JD, Draves KE, Gotoh Y, Krebs EG, Clark EA (2001) Both phosphorylation and caspase-mediated cleavage contribute to regulation of the Ste20-like protein kinase Mst1 during CD95/Fas-induced apoptosis. *J Biol Chem* **276:** 14909–14915

Guo C, Tommasi S, Liu L, Yee JK, Dammann R, Pfeifer GP (2007) RASSF1A is part of a complex similar to the *Drosophila* Hippo/Salvador/Lats tumor-suppressor network. *Curr Biol* **17:** 700–705

Irie HY, Pearline RV, Grueneberg D, Hsia M, Ravichandran P, Kothari N, Natesan S, Brugge JS (2005) Distinct roles of Akt1 and Akt2 in regulating cell migration and epithelial-mesenchymal transition. *J Cell Biol* **171:** 1023–1034

Jiang T, Qiu Y (2003) Interaction between Src and a C-terminal proline-rich motif of Akt is required for Akt activation. *J Biol Chem* **278:** 15789–15793

Kim MJ, Cardiff RD, Desai N, Banach-Petrosky WA, Parsons R, Shen MM, Abate-Shen C (2002) Cooperativity of Nkx3.1 and Pten loss of function in a mouse model of prostate carcinogenesis. *Proc Natl Acad Sci USA* **99:** 2884–2889

Koh H, Lee KH, Kim D, Kim S, Kim JW, Chung J (2000) Inhibition of Akt and its anti-apoptotic activities by tumor necrosis factor-induced protein kinase C-related kinase 2 (PRK2) cleavage. *J Biol Chem* **275:** 34451–34458

Kulik G, Klippel A, Weber MJ (1997) Antiapoptotic signalling by the insulin-like growth factor I receptor, phosphatidylinositol 3-kinase, and Akt. *Mol Cell Biol* **17:** 1595–1606

Li J, Yen C, Liaw D, Podsypanina K, Bose S, Wang SI, Puc J, Miliaresis C, Rodgers L, McCombie R, Bigner SH, Giovanella BC, Ittmann M, Tycko B, Hibshoosh H, Wigler MH, Parsons R (1997) PTEN, a putative protein tyrosine phosphatase gene mutated in human brain, breast, and prostate cancer. *Science* **275:** 1943–1947

Li L, Ren CH, Tahir SA, Ren C, Thompson TC (2003) Caveolin-1 maintains activated Akt in prostate cancer cells through scaffolding domain binding site interactions with and inhibition of serine/threonine protein phosphatases PP1 and PP2A. *Mol Cell Biol* **23:** 9389–9404

Lin J, Adam RM, Santiestevan E, Freeman MR (1999) The phosphatidylinositol 3′-kinase pathway is a dominant growth factor-activated cell survival pathway in LNCaP human prostate carcinoma cells. *Cancer Res* **59:** 2891–2897

Maira SM, Galetic I, Brazil DP, Kaech S, Ingley E, Thelen M, Hemmings BA (2001) Carboxyl-terminal modulator protein (CTMP), a negative regulator of PKB/Akt and v-Akt at the plasma membrane. *Science* **294:** 374–380

Majumder PK, Sellers WR (2005) Akt-regulated pathways in prostate cancer. *Oncogene* **24:** 7465–7474

Nichols BJ (2003) GM1-containing lipid rafts are depleted within clathrin-coated pits. *Curr Biol* **13:** 686–690

Oh HJ, Lee KK, Song SJ, Jin MS, Song MS, Lee JH, Im CR, Lee JO, Yonehara S, Lim DS (2006) Role of the tumor suppressor RASSF1A in Mst1-mediated apoptosis. *Cancer Res* **66:** 2562–2569

O'Neill E, Rushworth L, Baccarini M, Kolch W (2004) Role of the kinase MST2 in suppression of apoptosis by the proto-oncogene product Raf-1. *Science* **306:** 2267–2270

Praskova M, Khoklatchev A, Ortiz-Vega S, Avruch J (2004) Regulation of the MST1 kinase by autophosphorylation, by the growth inhibitory proteins, RASSF1 and NORE1, and by Ras. *Biochem J* **381:** 453–462

Sable CL, Filippa N, Filloux C, Hemmings BA, Van Obberghen E (1998) Involvement of the pleckstrin homology domain in the insulin-stimulated activation of protein kinase B. *J Biol Chem* **273:** 29600–29606

Sarbassov DD, Ali SM, Sengupta S, Sheen JH, Hsu PP, Bagley AF, Markhard AL, Sabatini DM (2006) Prolonged rapamycin treatment inhibits mTORC2 assembly and Akt/PKB. *Mol Cell* **22:** 159–168

Schlesinger TK, Bonvin C, Jarpe MB, Fanger GR, Cardinaux JR, Johnson GL, Widmann C (2002) Apoptosis stimulated by the 91-kDa caspase cleavage MEKK1 fragment requires translocation to soluble cellular compartments. *J Biol Chem* **277:** 10283–10291

Skaletz-Rorowski A, Lutchman M, Kureishi Y, Lefer DJ, Faust JR, Walsh K (2003) HMG-CoA reductase inhibitors promote cholesterol-dependent Akt/PKB translocation to membrane domains in endothelial cells. *Cardiovasc Res* **57:** 253–264

Solomon KR, Mallory MA, Finberg RW (1998) Determination of the non-ionic detergent insolubility and phosphoprotein associations of glycosylphosphatidylinositol-anchored proteins expressed on T cells. *Biochem J* **334** (Part 2)**:** 325–333

Trotman LC, Alimonti A, Scaglioni PP, Koutcher JA, Cordon-Cardo C, Pandolfi PP (2006) Identification of a tumour suppressor network opposing nuclear Akt function. *Nature* **441:** 523–527

Udan RS, Kango-Singh M, Nolo R, Tao C, Halder G (2003) Hippo promotes proliferation arrest and apoptosis in the Salvador/Warts pathway. *Nat Cell Biol* **5:** 914–920

Ura S, Masuyama N, Graves JD, Gotoh Y (2001) Caspase cleavage of MST1 promotes nuclear translocation and chromatin condensation. *Proc Natl Acad Sci USA* **98:** 10148–10153

Wang R, Brattain MG (2006) AKT can be activated in the nucleus. *Cell Signal* **18:** 1722–1731

Widmann C, Gibson S, Johnson GL (1998) Caspase-dependent cleavage of signaling proteins during apoptosis. A turn-off mechanism for anti-apoptotic signals. *J Biol Chem* **273:** 7141–7147

Yamamoto S, Yang G, Zablocki D, Liu J, Hong C, Kim SJ, Soler S, Odashima M, Thaisz J, Yehia G, Molina CA, Yatani A, Vatner DE, Vatner SF, Sadoshima J (2003) Activation of Mst1 causes dilated cardiomyopathy by stimulating apoptosis without compensatory ventricular myocyte hypertrophy. *J Clin Invest* **111:** 1463–1474

Yoeli-Lerner M, Yiu GK, Rabinovitz I, Erhardt P, Jauliac S, Toker A (2005) Akt blocks breast cancer cell motility and invasion through the transcription factor NFAT. *Mol Cell* **20:** 539–550

Zhuang L, Kim J, Adam RM, Solomon KR, Freeman MR (2005) Cholesterol targeting alters lipid raft composition and cell survival in prostate cancer cells and xenografts. *J Clin Invest* **115:** 959–968

Zhuang L, Lin J, Lu ML, Solomon KR, Freeman MR (2002) Cholesterol-rich lipid rafts mediate akt-regulated survival in prostate cancer cells. *Cancer Res* **62:** 2227–2231

